

Kinetics of Electron Transfer Reaction between Co(II) and Chlorate Ions: Experimental and Modeling Study

Mahwish Mobeen Khan and Syed Mumtaz Danish Naqvi*

Department of Applied Chemistry & Chemical Technology, University of Karachi, Karachi-75270, Pakistan.

mmobeen@uok.edu.pk

(Received on 2nd March 2021, accepted in revised form 26th August 2021)

Summary: This research article reports original experimental and modeling detail of kinetics of the electron transfer reaction between Co(II) and chlorate ions in acetic acid solution. Design of experiment methodology has been employed to elucidate the effects of temperature and initial concentrations of reactants on the rate of reaction. Levenberg-Marquardt method has been used to fit processed kinetic data (temperatures, initial concentrations of reactants, and concentrations and rates of production of Co(III)) on to various possible rate equations. This algorithm provides a proficient mean for compensating the capricious effects of the experimental process variables and results in the maximum likelihood estimates of the kinetic parameters. The most significant rate law has been selected, on the basis of statistical analyses of the residuals between the predicted and experimental rates. The analyses suggest that the intrinsic rate of reaction is proportional to first power of chlorate concentration but for Co(II) the order is fractional ($0.7455 \approx \frac{3}{4}$). The effect of temperature on the observed rate constant (precision = 0.02 %) is excellently described by the Arrhenius and Eyring equations and the sluggish nature of the reaction is clearly manifested by the high energy (> 93 kJ/mol), negative entropy (-28.5286 J/mol-K) and very small equilibrium constant of activation. Further fairly negative standard entropy of activation shows there is usually considerable rearrangement of energy among various degrees of freedom during the formation of activated complex and proposes an associative mechanism for formation of the activated complex. This research is performed to develop a kinetic model for the electron transfer reaction between Co(II) and chlorate ion. As a result, a redox couple of Co(II)/Co(III) has been formed which is used as a potent oxidation catalyst in chemical industries.

Keywords: Chemical kinetics, Electron transfer reaction, Kinetic modelling, Cobalt (II)/(III).

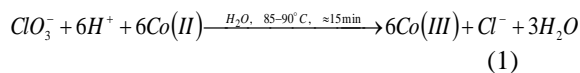
Introduction

There are numerous examples of industrial and academic importance that typically employ fragile transition metal complexes either as catalysts or as stoichiometric reagents. Among the transition metal complexes that have been described, the complexes of cobalt have received special attention. As a matter of fact by the end of 2011, there had been approximately 6100 reports on cobalt acetate alone. Generally, acetate complexes of cobalt are important as oxidation catalysts in acetic acid. One such example of industrial importance is homogeneous catalytic autoxidation of hydrocarbons with molecular oxygen that has been practiced on huge scales. A free-radical chain mechanism governs this reaction network, resulting in hydroperoxides as intermediate that are catalytically decomposed in the presence of Co(III)/Co(II) redox couple, generating free radicals for propagation and thus accelerates the normal autoxidation process.[1-9].

The starting species in several of the homogeneous catalytic autoxidation systems is Co(II), which is oxidized in-situ to Co(III) and thus forms the catalytic redox couple. However, there are examples wherein either Co(III) or readymade redox couple Co(III)/Co(II) has also been employed. The

presence of an initial amount of Co(III) is always advantageous as not only it promotes the initiation by direct electron transfer from C-H bonds to Co(III) resulting in instantaneous appearance of hydroperoxides in the presence of molecular oxygen but at the same time, in combination with Co(II), it provides the catalytic driving force for decomposition of hydroperoxides to final products at an appreciable and economical rate.[10-33].

Due to the natural utility of Co(III) as an initiator and catalyst, easy and economical synthetic route for Co(III) is highly desirable. Compilation of many oxidative routes from Co(II) to Co(III) are available in the literature, most of them involving expensive reagents and complicated apparatus and consist of laborious preparation and purification steps.⁵ However, a novel, simple, and economical one step possibility was qualitatively described elsewhere by one of the authors that consists of treating the acetic acid solution of cobalt(II)acetate tetrahydrate with aqueous potassium chlorate according to the following ionic reaction:[30,32].



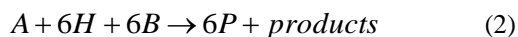
*To whom all correspondence should be addressed.

It has been characterized during several scientific studies that the catalytic species of cobalt in acetic acid are pink Co(II) = $\text{Co}(\text{Ac})_2(\text{HAc})_m(\text{H}_2\text{O})_n$ and dark green Co(III) = $[\text{Co}_3\text{O}(\text{OAc})_6(\text{HOAc})_3]^+$ + $[\text{Co}_3\text{O}(\text{OAc})_5(\text{OH})(\text{HOAc})_3]^+$ [34-42]. Therefore for simplicity, complex species of cobalt will be written as Co(II) and Co(III) throughout in this article. Actually the electron transfer from high-spin Co(II) to chlorate to yield low-spin Co(III) is a slow process [43]. Same has been the practical observation during the present study that makes it convenient to follow reaction (1) in the time domain by the usual analytical tools used in chemical kinetics studies.

Reaction (1), hereinafter termed as the reaction system, offers the flexibility of preparing quantitative amounts of the redox couple Co(III)/Co(II) of exactly known composition, by altering the initial amounts of the reactants. This is possible if the intrinsic kinetic fingerprints of the reaction system are discovered in the form of a rate law. Accordingly, the present work aims at the detailed kinetic study of the reaction system from the experimental and fitting aspects. This practical possibility has been entirely readdressed from the kinetic point of view during the present study and novel kinetic results are presented in this article for electron transfer reaction between Co(II) and chlorate ions in acetic acid solution.

Theoretical Details

If $A = \text{ClO}_3^-$, $H = \text{H}^+$, $B = \text{Co(II)}$ and $P = \text{Co(III)}$, then for the purpose of kinetic study, the reaction system may simply be written as:



The rate of consumption of A in the reaction system may be expressed as:

$$-\frac{dC_A}{dt} = k_c C_H^\gamma C_A^\alpha C_B^\beta \quad (3)$$

where, α , β and γ are the orders of reaction with respect to A , B and H respectively. Since the reaction between very dilute A and B is carried out in acetic acid, therefore there is always an abundant supply of H , as a result of the dissociation of acetic acid. Factually there is always negligible difference in the pH of the reaction mixture at the start and after substantial time allowed for the reaction. Hence for the sake of simplicity equation (3) may be written as:

$$-\frac{dC_A}{dt} = k' C_A^\alpha C_B^\beta \quad (4)$$

where the rate constant $k' = k_c C_H^\gamma$

Equation (4) may be written in an alternative form by considering the stoichiometry of the reaction system and according to the Arrhenius equation:[44]

$$r = \frac{dC_P}{dt} = 6A_a e^{-E_a/RT} \left(C_{A_0} - \frac{C_P}{6} \right)^\alpha (C_{B_0} - C_P)^\beta \quad (5)$$

where the observed rate constant $k = 6k' = 6A_a e^{-E_a/RT}$

Non-linear ordinary differential equation (5) describes the simultaneous effect of temperature and concentration of Co(III) upon the rate of production thereof and has been used as the rate law during the present study to fit the experimental kinetic data. The fitting of kinetic data results in the estimated values for the orders of reaction with respect to the reactants as well as estimated values for pre-exponential factor A_a and energy of activation E_a in the Arrhenius equation.

The estimated values for Arrhenius parameters are used to estimate the observed rate constants k for the reaction system at various temperatures. The observed rate constants are then subjected to Eyring analysis based on the Eyring equation that has roots in the activated complex theory and quantum mechanics, to provide an alternative definition for the effect of absolute temperature on the observed rate constant:[45,46]

$$k = \frac{k_B T}{h} e^{-\Delta G^\ddagger/RT} \quad (6)$$

The standard Gibbs energy of activation ΔG^\ddagger is in turn defined in terms of standard enthalpy ΔH^\ddagger and entropy ΔS^\ddagger of activation as:

$$\Delta G^\ddagger = \Delta H^\ddagger - T\Delta S^\ddagger \quad (7)$$

$$\text{Hence, } k = \frac{k_B T}{h} e^{\frac{\Delta S^\ddagger}{R}} e^{-\frac{\Delta H^\ddagger}{RT}} \quad (8)$$

Eyring analysis consists of fitting $\ln(k/T)$ against $1/T$. The slope and intercept of the linear form of equation (8) gives the estimates for ΔH^\ddagger and ΔS^\ddagger . The sign and magnitude of ΔS^\ddagger provides valuable information about the nature of the activated complex formed during a reaction. Since, in terms of equilibrium constant, ΔG^\ddagger may alternatively be defined as:

$$\Delta G^\ddagger = -RT \ln K^\ddagger \quad (9)$$

Hence using equations (7) and (9) the equation for the equilibrium constant K^\ddagger for the formation of activated complex may be written as:

$$K^\ddagger = e^{\frac{T\Delta S^\ddagger - \Delta H^\ddagger}{RT}} \quad (10)$$

Experimental

A significant part of this academic research has been dealt with the collection of experimental kinetic data for the reaction system. Such kinetic data consist of the concentrations of Co(III) in the time domain and the corresponding rates of production thereof as function of temperature and initial concentrations of the reactants.

Materials.

Chemical reagents, Cobalt(II) acetate tetrahydrate (AR) (6147-53-1), potassium chlorate (AR) (3811-04-9), potassium iodate (AR) (7758-05-6), potassium iodide (EP) (7681-11-0), sodium carbonate (EP) (497-19-8), sodium thiosulfate (EP) (10102-17-7), iso-propanol (EP) (67-63-0) and acetic acid (64-19-7) were purchased from various suppliers and were used in general without any further treatment. Double distilled water was produced using Hamilton double distillation water still.

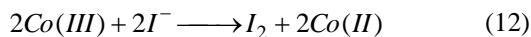
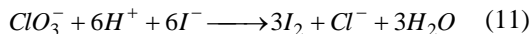
Safety

Potassium chlorate is an irritant and strong oxidizing agent. However, dilute neutral aqueous solution of potassium chlorate is safe. As chlorate is reduced to chloride in the reaction system so it will not become an environmental hazard. On the other hand, Cobalt(II) acetate tetrahydrate is irritant and mutagen while acetic acid is corrosive.

Quenching mixture (QM)

The reaction system is strongly pH dependent and sweeps smoothly in acetic acid (pH = 1 – 2). However, for the purpose of following the reaction in the time domain it is necessary to virtually

stop the reaction. Further during the iodometric determination of Co(III) in a low pH reaction mixture, chlorate would strongly interfere as it has a pronounced tendency over Co(III) to oxidize iodide ions according to following ionic reactions:



In fact major part of the iodide ions (molar ratio 3:1 for chlorate to Co(III)) would be consumed by chlorate if not properly masked in a system of low pH containing both chlorate and Co(III). Both these requirements may be fulfilled by properly buffering the reaction mixture at a pH of 4 – 5. In this pH range chlorate would practically be unable to oxidize either Co(II) or iodide ions.⁴⁷ For that reasons, quenching mixture (QM) should have the simultaneous ability to virtually stop the main reaction system and not to interfere with Co(III) for the precise iodometric determination of Co(III).

The buffering QM is prepared by digesting calculated amount of sodium carbonate (572 g) and acetic acid (624 mL) in the presence of some double distilled water under constant stirring and mild heating. The resulting solution is boiled to expel carbon dioxide. Calculated amount of potassium iodide (18 g) is added and the solution is made up to 2.0 L with double distilled water (Supporting Information). When reaction mixture is quenched with equal volume of this QM it gives a pH of 4 – 5. During kinetic experiments some crystallization occurs in the QM at room temperature. To get rid of this the QM flask is always put on a hot plate during the kinetic runs and the preheated QM is taken in the jacketed transfer funnel maintained at 333.15K (Section 3.4).

Experimental rig

An approximately 50 ml jacketed Pyrex glass reaction vessel, hereinafter called the reactor, has been fabricated as a core part of the experimental rig (Fig. 1). Another jacketed Pyrex glass transfer funnel is placed over one of the three inlets to deliver QM. Both the reactor and the transfer funnel are connected to two thermostatic circulating baths for maintaining isothermal conditions within the reactor and for delivering the QM at a constant temperature of 333.15K. The other two inlets have been used one for a thermometer and the other for a micro burette to deliver titrant (standard solution of sodium thiosulfate). Constant stirring within the reactor has been provided with a magnetic stirrer beneath the reactor.

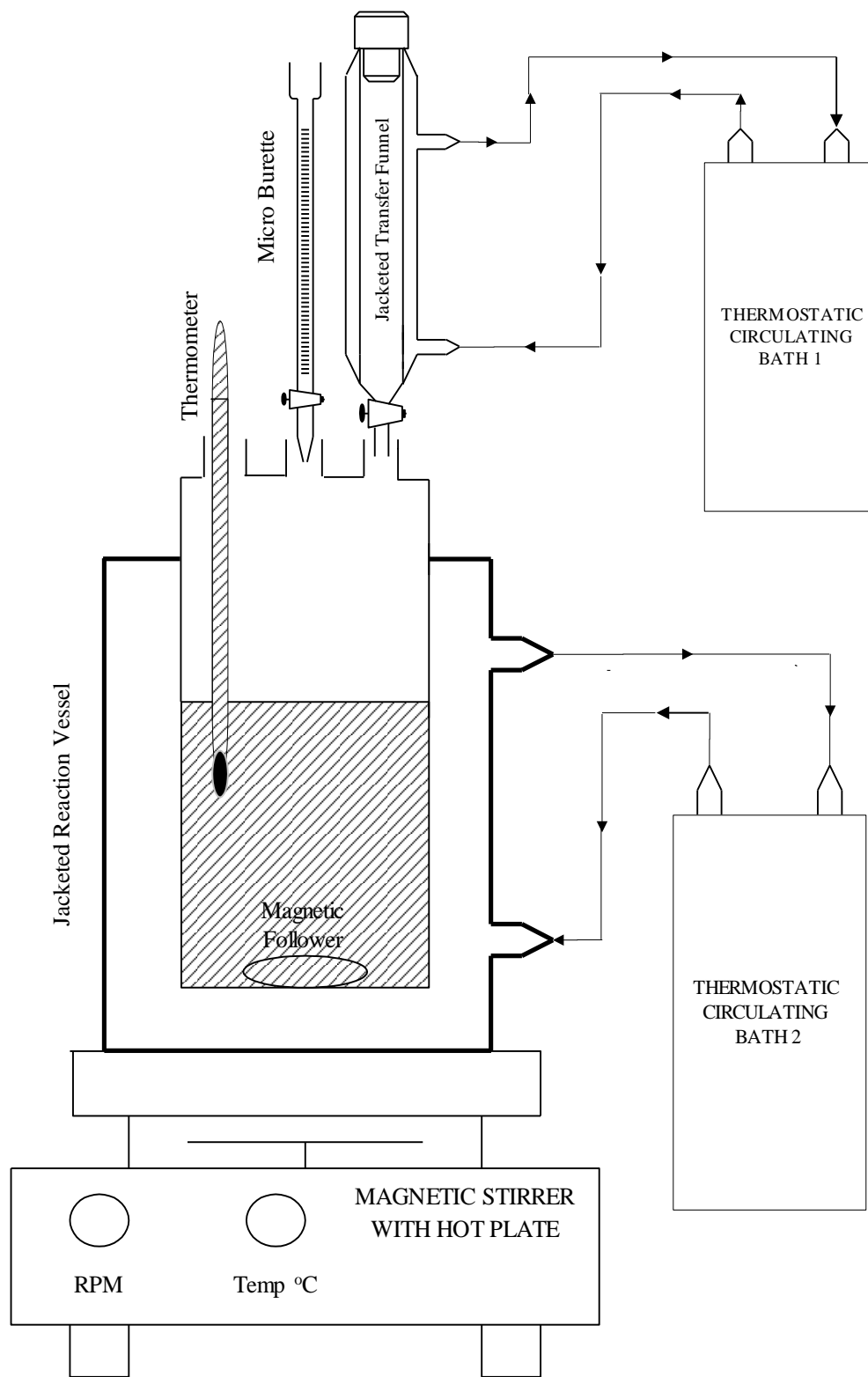


Fig. 1: Schematic diagram of experimental rig.

Design of experiment (DOE)

A design of experiment (DOE) methodology has been used to vary the initial concentrations of Co(II) and chlorate in a systematic way during kinetic experiments. The coded DOE has been constructed by stacking 25 rows for partial factorial design of two variables at 5 levels, 8 rows of star design at 4 levels, and 4 replicates in the center, all at 358.15K, and 11 replicates at various other temperatures making a total of 48 experiments (Table-1). Partial factorial design was chosen to increase the number of levels without having excessive number of experiments, as is usual with the multilevel full factorial designs. At the same time, it provides with a statistically orthogonal design in which there is no correlation between the factors [48,49].

The coded DOE has been transformed to practical scale by carefully solving the mass balance equations of the reaction system for the volumes of reactants and solvent required for preparation of the reaction mixture (Supporting Information). The result is a perfectly orthogonal design in which all the points are laid symmetrically on a rectangle, forming perfect right angles, and hence there is no correlation between the initial concentrations of reactants used in subsequent kinetic data fitting (Fig. 2).

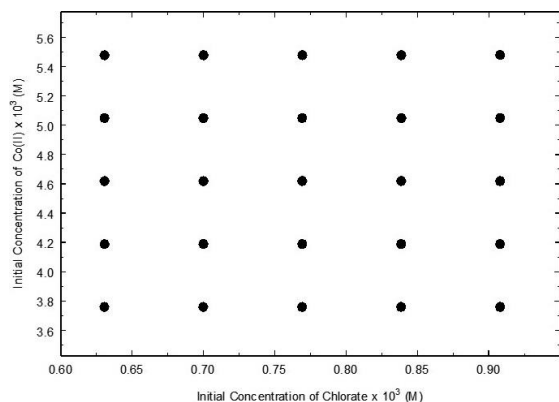


Fig 2: Orthogonal design for kinetic experiments.

Kinetic experiments

Reaction mixtures were prepared according to the real DOE (Table 1). Calculated volumes of Co(II) solution and acetic acid were taken in test tubes by the help of burettes. The test tubes were put in a thermostatic bath to preheat the reaction mixture up to the reaction temperature. After fifteen minutes the contents of the test tube were carefully transferred to the reactor also maintained at reaction temperature.

After five more minutes the reaction system was initiated by transferring calculated volume of potassium chlorate solution using a micro transfer pipette and at the same time stopwatch was started. After a specified time, the reaction was quenched with preheated QM and simultaneously the stopwatch was stopped.

Analysis of reaction mixture

The quenched reaction mixture was analyzed for its Co(III) content. The liberated iodine was titrated against standard sodium thiosulfate (prepared in 1:1 isopropanol-water mixture and standardized against iodate-iodide system) [30,32] to a violet end point that is color of Co(II) in the presence of excess acetate in acetic acid [34]. The expression for the experimental concentration of Co(III) $C_{P_{Exp}}$ would be:

$$C_{P_{Exp}} = \frac{C_{S_2O_3^{-2}} V_{S_2O_3^{-2}}}{V_{RM}} \quad (13)$$

Kinetic data

Ample raw kinetic data (590 data points from 5 – 300s and from 338.15K – 363.15K) were collected through careful experimental procedure described above. Such raw data include $C_{P_{Exp}}$ and t_{Exp} (Fig. 3). In majority of cases, except for set T1 – T3, raw kinetic data have been smoothed using generalized exponential functions so that processed concentration of Co(III) C_P could be expressed as:

$$C_P = b_0 e^{b_1 t} + b_2 \quad (14)$$

Consequently rate of production of Co(III) is:

$$r = b_0 b_1 e^{b_1 t} \quad (15)$$

In few instances where there is a brief initial induction period (set T1 – T3) raw kinetic data have been smoothed using generalized logistic functions of the form:

$$C_P = \frac{b_0}{1 + b_1 e^{-b_2 t}} \quad (16)$$

$$\text{So that, } r = \frac{b_0 b_1 b_2 e^{-b_2 t}}{(1 + b_1 e^{-b_2 t})^2} \quad (17)$$

In equations (14) – (17), b_0 , b_1 and b_2 are adjustable parameters found through least squares fitting of raw kinetic data. The precision in the measurement of C_p can be observed in Fig. 4.

A subset of 570 kinetic data points were selected for fitting, from a total of 720 data points computed using equations (14) – (17). This subset consists of 495 data points according to DOE studied at 358.15K and remaining are at various other

temperatures (353.15, 356.15, 360.15, 362.15 and 363.15K) and at the center of the DOE (Fig. 5). The selection of temperature range for kinetic data fitting was based on the analysis of r at 5s for various temperatures from 338.15 – 363.15K (Fig. 6). Below and at 338.15K r is almost negligible and even up to 348.15K the rate is not appreciable. Beyond 348.15K the rate begins to increase and between 353.15 – 363.15K there is a smooth rise in the rate. Therefore temperature range of 353.15 – 363.15K was selected for kinetic data fitting purpose as in this range the rate is appreciably variable.

Table-1: Design of Experiments (DOE).

| Set # | Coded DOE (Factors) | | Real DOE | | | | |
|-------|---------------------|----|----------|--------------------------------------|---------------------------------|-----------------------|---|
| | x1 | x2 | T (K) | KClO ₃ (Aqueous) (0.23 M) | Co(II)Ac (Acetic Acid) (0.05 M) | Acetic Acid (Solvent) | Na ₂ S ₂ O ₃ (Titrant) |
| | | | | (□L) | (mL) | (mL) | (mM) |
| 1 | 0 | 0 | 358.15 | 83.3 | 2.30 | 20.8 | 23 |
| 2 | 0 | -2 | 358.15 | 83.3 | 2.73 | 20.4 | 23 |
| 3 | -2 | -2 | 358.15 | 68.3 | 2.73 | 20.4 | 23 |
| 4 | -2 | 2 | 358.15 | 68.3 | 1.87 | 21.3 | 23 |
| 5 | 2 | -1 | 358.15 | 98.3 | 2.51 | 20.6 | 23 |
| 6 | -1 | 2 | 358.15 | 75.8 | 1.87 | 21.3 | 23 |
| 7 | 2 | 0 | 358.15 | 98.3 | 2.30 | 20.8 | 23 |
| 8 | 0 | -1 | 358.15 | 83.3 | 2.51 | 20.6 | 23 |
| 9 | -1 | -1 | 358.15 | 75.8 | 2.51 | 20.6 | 23 |
| 10 | -1 | 1 | 358.15 | 75.8 | 2.09 | 21.0 | 23 |
| 11 | 1 | 2 | 358.15 | 90.8 | 1.87 | 21.2 | 23 |
| 12 | 2 | 1 | 358.15 | 98.3 | 2.09 | 21.0 | 23 |
| 13 | 1 | 0 | 358.15 | 90.8 | 2.30 | 20.8 | 23 |
| 14 | 0 | 2 | 358.15 | 83.3 | 1.87 | 21.2 | 23 |
| 15 | 2 | 2 | 358.15 | 98.3 | 1.87 | 21.2 | 23 |
| 16 | 2 | -2 | 358.15 | 98.3 | 2.73 | 20.4 | 23 |
| 17 | -2 | 1 | 358.15 | 68.3 | 2.09 | 21.0 | 23 |
| 18 | 1 | -2 | 358.15 | 90.8 | 2.73 | 20.4 | 23 |
| 19 | -2 | 0 | 358.15 | 68.3 | 2.30 | 20.8 | 23 |
| 20 | 0 | 1 | 358.15 | 83.3 | 2.09 | 21.0 | 23 |
| 21 | 1 | 1 | 358.15 | 90.8 | 2.09 | 21.0 | 23 |
| 22 | 1 | -1 | 358.15 | 90.8 | 2.51 | 20.6 | 23 |
| 23 | -1 | -2 | 358.15 | 75.8 | 2.73 | 20.4 | 23 |
| 24 | -2 | -1 | 358.15 | 68.3 | 2.51 | 20.6 | 23 |
| 25 | -1 | 0 | 358.15 | 75.8 | 2.30 | 20.8 | 23 |
| 26 | -2 | 0 | 358.15 | 68.3 | 2.30 | 20.8 | 23 |
| 27 | -1 | 0 | 358.15 | 75.8 | 2.30 | 20.8 | 23 |
| 28 | 1 | 0 | 358.15 | 90.8 | 2.30 | 20.8 | 23 |
| 29 | 2 | 0 | 358.15 | 98.3 | 2.30 | 20.8 | 23 |
| 30 | 0 | -2 | 358.15 | 83.3 | 2.73 | 20.4 | 23 |
| 31 | 0 | -1 | 358.15 | 83.3 | 2.51 | 20.6 | 23 |
| 32 | 0 | 1 | 358.15 | 83.3 | 2.09 | 21.0 | 23 |
| 33 | 0 | 2 | 358.15 | 83.3 | 1.87 | 21.2 | 23 |
| 34 | 0 | 0 | 358.15 | 83.3 | 2.30 | 20.8 | 23 |
| 35 | 0 | 0 | 358.15 | 83.3 | 2.30 | 20.8 | 23 |
| 36 | 0 | 0 | 358.15 | 83.3 | 2.30 | 20.8 | 23 |
| 37 | 0 | 0 | 358.15 | 83.3 | 2.30 | 20.8 | 23 |
| T1 | 0 | 0 | 338.15 | 83.3 | 2.30 | 20.8 | 23 |
| T2 | 0 | 0 | 343.15 | 83.3 | 2.30 | 20.8 | 23 |
| T3 | 0 | 0 | 348.15 | 83.3 | 2.30 | 20.8 | 23 |
| T4 | 0 | 0 | 350.15 | 83.3 | 2.30 | 20.8 | 23 |
| T5 | 0 | 0 | 351.15 | 83.3 | 2.30 | 20.8 | 23 |
| T6 | 0 | 0 | 352.15 | 83.3 | 2.30 | 20.8 | 23 |
| T7 | 0 | 0 | 353.15 | 83.3 | 2.30 | 20.8 | 23 |
| T8 | 0 | 0 | 356.15 | 83.3 | 2.30 | 20.8 | 23 |
| T9 | 0 | 0 | 360.15 | 83.3 | 2.30 | 20.8 | 23 |
| T10 | 0 | 0 | 362.15 | 83.3 | 2.30 | 20.8 | 23 |
| T11 | 0 | 0 | 363.15 | 83.3 | 2.30 | 20.8 | 23 |

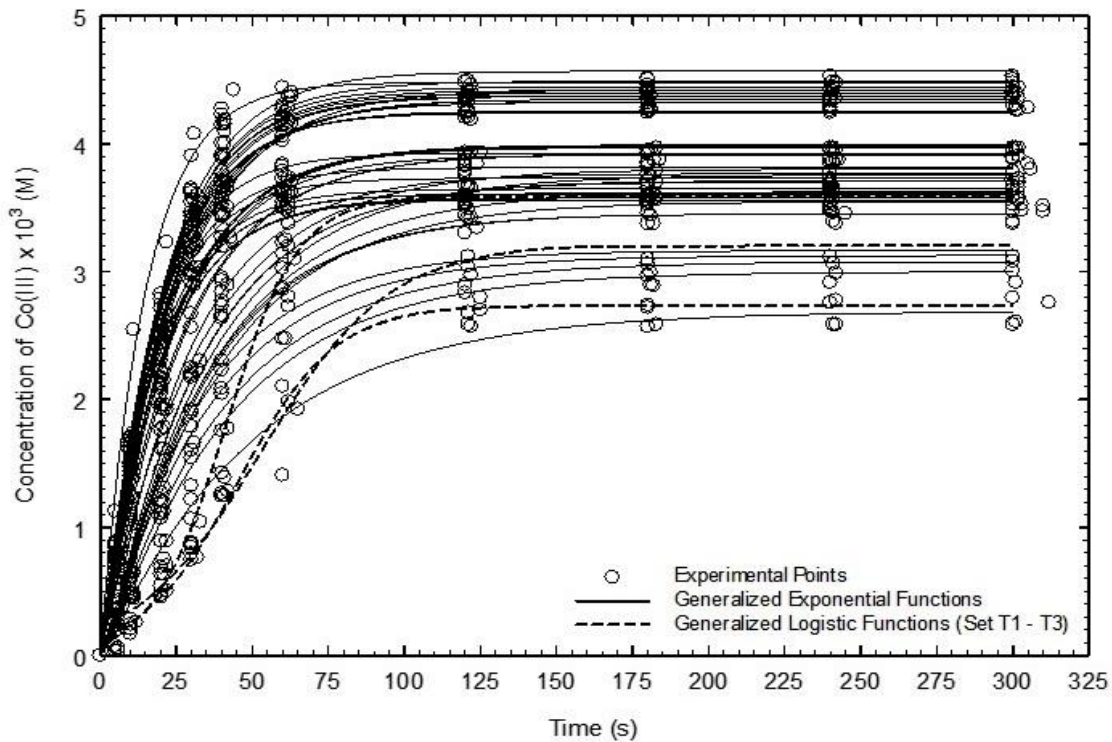


Fig 3: Collective experimental kinetic data.

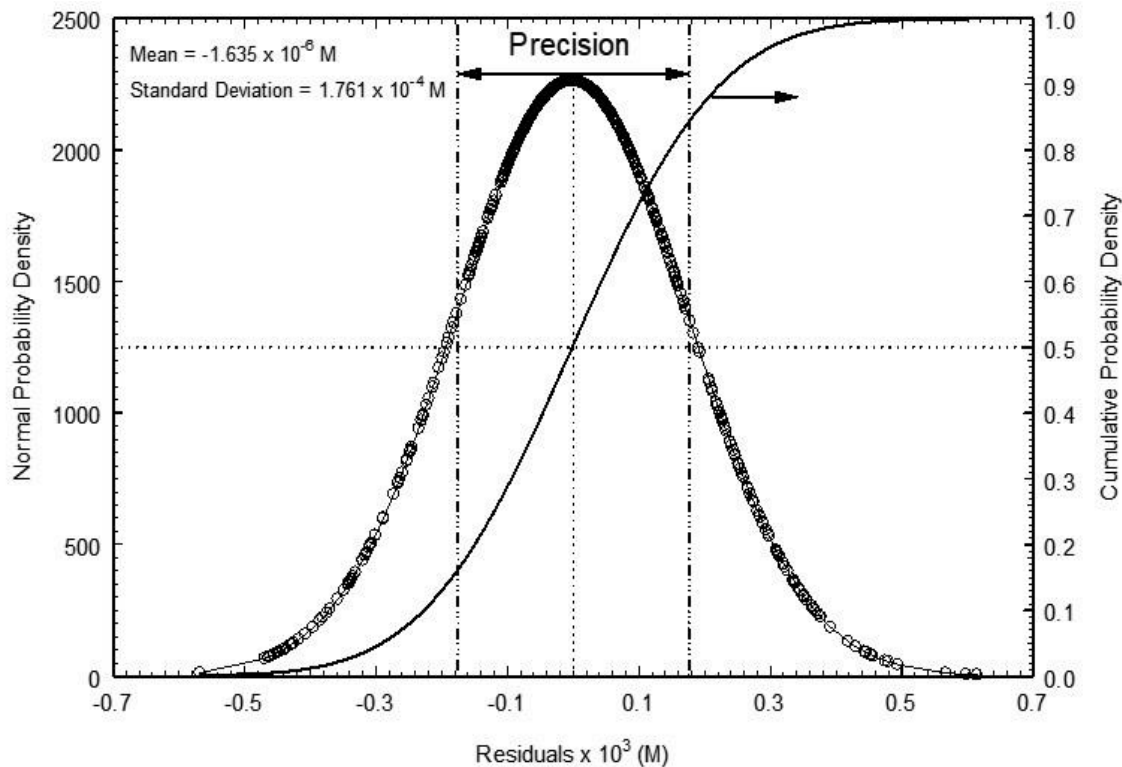


Fig 4: Precision in the measurement of C_p .

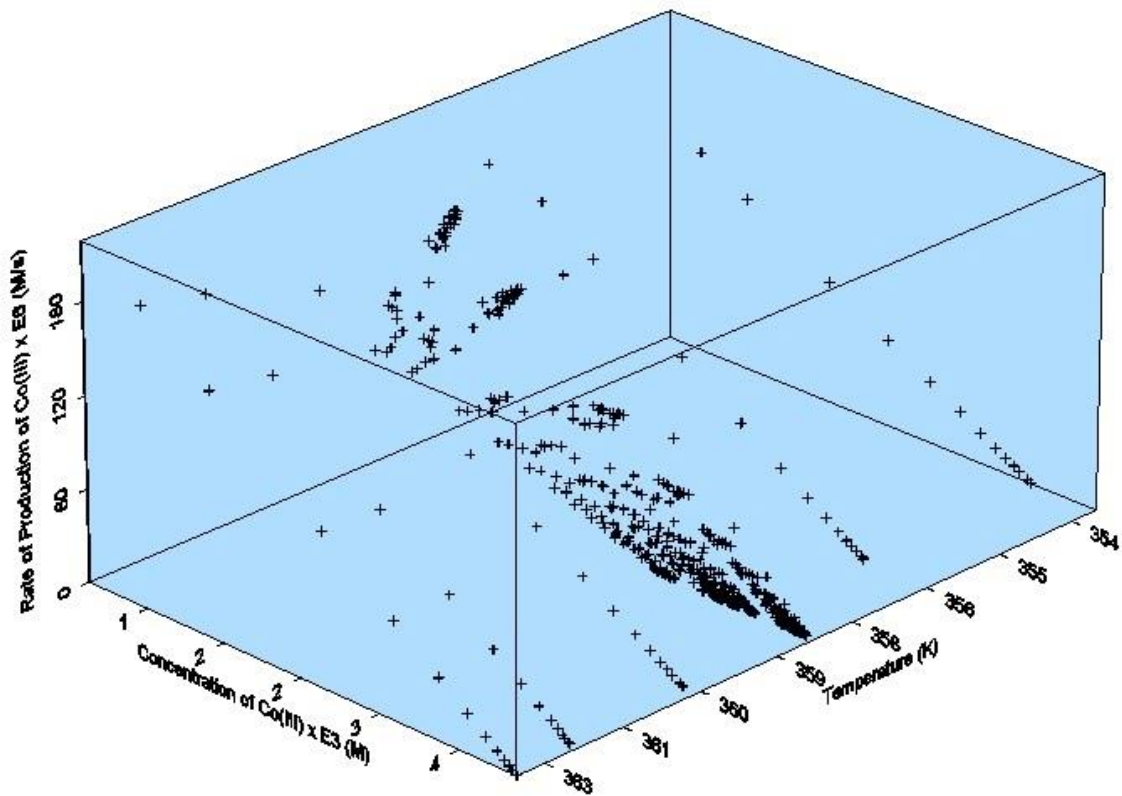


Fig 5: Processed kinetic data for fitting.

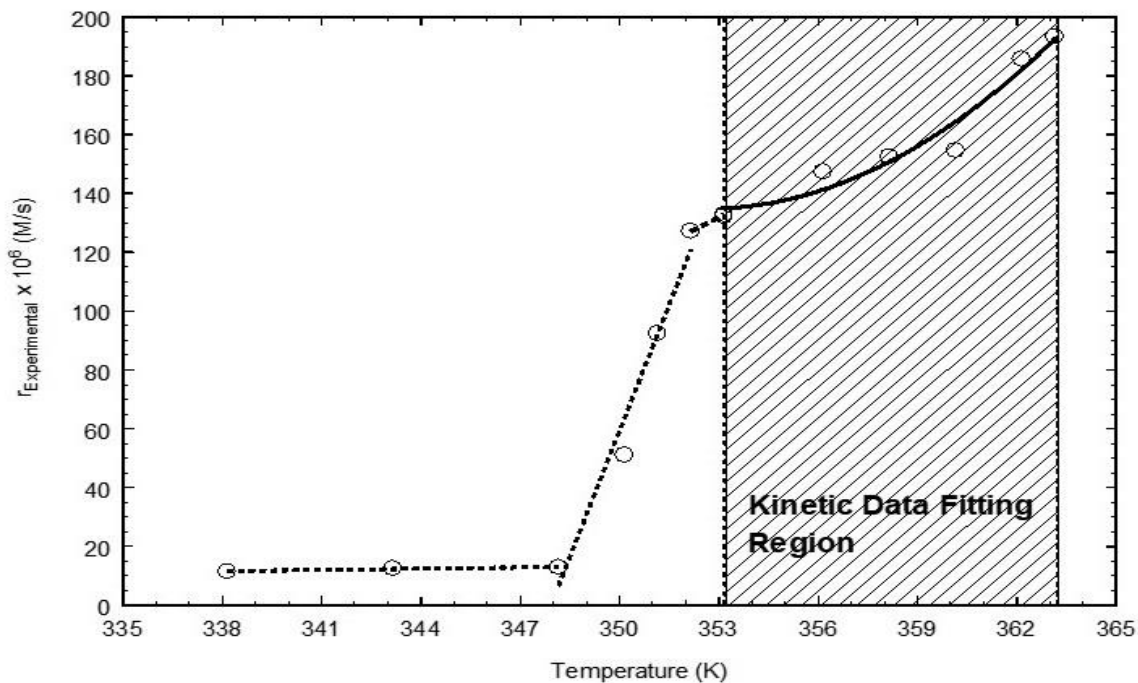


Fig 6: Effect of temperature on the rate of production of Co(III) at 5 s and at the center of the DOE.

RLB all four kinetic parameters were considered as unknown during kinetic data fitting. The estimated kinetic parameters and the analysis of variance are contained in Table 2 and 4. The predicted rates of reaction against the corresponding experimental values have been compiled in Fig. 7. The associated residual analysis can be observed in Fig. 8. As can be seen a reasonable bit of improvement over RLA was achieved but still the fitting was not fair enough. However, at least it had been established that $\alpha = 0.9590 \approx 1$ i.e., chlorate follows an almost clean first order consumption during the reaction but order for the consumption of Co(II) was still far from unity. It was concluded that if another variant for equation (5), namely RLC is tried with $\alpha = 1$ and

manually adjusting β by hit and trial a reasonable rate law could be discovered that simulates the experimental kinetic data accurately. Thus only A_a and E_a were considered as unknown, α was fixed at 1 and β was manually varied during kinetic data fitting with RLC. As a result, a rate law has been built, which has an immaculate tendency to accurately describe the kinetic behavior of reaction system. The details of kinetic and statistical analyses for RLC are contained in Table- 2 and 5 and Figs 7 and 8.

Table-2: Estimated kinetic parameters of the reaction system.

| | RLA | RLB | RLC |
|--|------------|------------|------------|
| α | 1.0000 | 0.9590 | 1.0000 |
| β | 1.0000 | 0.9111 | 0.7455 |
| A_a | 9.0900E+13 | 7.3520E+13 | 9.6140E+13 |
| E_a (kJ/mol) | 88.935 | 90.686 | 93.372 |
| ΔH^\ddagger (kJ/mol) | 86.205 | 87.955 | 90.642 |
| $ARE = \left \frac{E_a - \Delta H^\ddagger}{E_a} \right $ (%) | 3.0700 | 3.0100 | 2.9200 |
| $ARE = \left \frac{E_a - \text{mean}(\Delta H^\ddagger + RT)}{E_a} \right $ (%) | 0.1145 | 0.1123 | 0.1091 |
| ΔS^\ddagger (J/mol-K) | -28.063 | -26.298 | -28.529 |

Table 3: Analysis of variance (RLA).

| | Degrees of Freedom | Sum of Squares | Mean Sum of Squares |
|-------------|--------------------|----------------|---------------------|
| Regression | 570 | 1.1600E-6 | 2.0350E-9 |
| Residual | 567 | 1.7800E-7 | 3.1400E-10 |
| Total | 1137 | 1.3380E-6 | 1.1770E-9 |
| F_{ratio} | 6.4820 | R^2 | 0.8670 |
| P_{value} | 0.0000 | $RMSD$ | 1.7672E-5 |

Table 4: Analysis of variance (RLB).

| | Degrees of Freedom | Sum of Squares | Mean Sum of Squares |
|-------------|--------------------|----------------|---------------------|
| Regression | 570 | 1.1380E-6 | 1.9970E-9 |
| Residual | 565 | 1.6340E-7 | 2.8920E-10 |
| Total | 1135 | 1.3010E-6 | 1.1470E-9 |
| F_{ratio} | 6.9032 | R^2 | 0.8744 |
| P_{value} | 0.0000 | $RMSD$ | 1.6932E-5 |

Table-5: Analysis of variance (RLC).

| | Degrees of Freedom | Sum of Squares | Mean Sum of Squares |
|-------------|--------------------|----------------|---------------------|
| Regression | 570 | 1.0900E-6 | 1.9120E-9 |
| Residual | 567 | 1.4470E-7 | 2.5510E-10 |
| Total | 1137 | 1.2340E-6 | 1.0860E-9 |
| F_{ratio} | 7.4923 | R^2 | 0.8828 |
| P_{value} | 0.0000 | $RMSD$ | 1.5931E-5 |

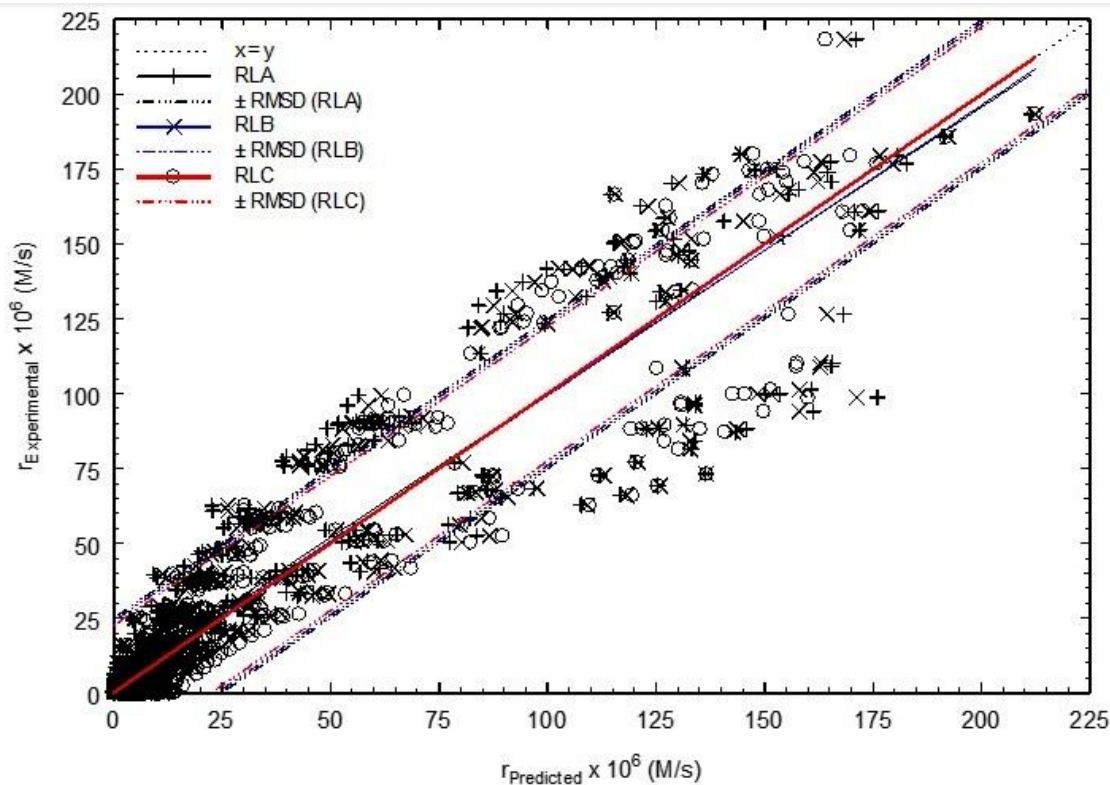


Fig 7: Comparison of the different variants of rate law and the ideal response of the reaction system.

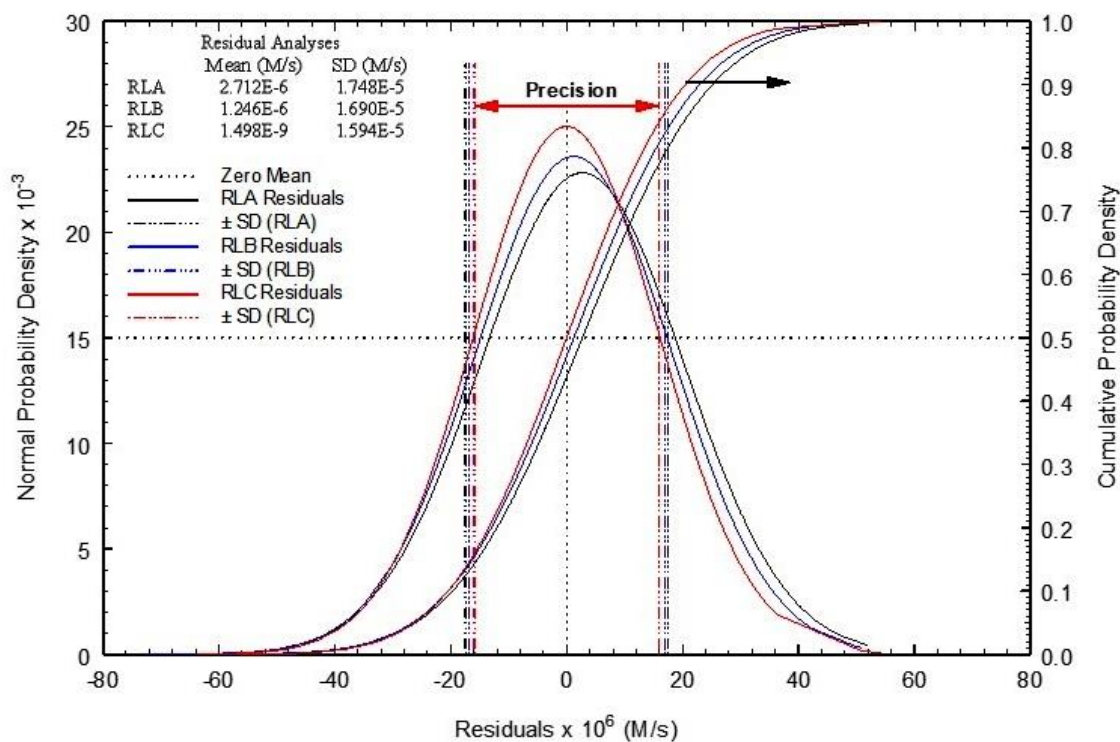


Fig 8: Precision analyses of the different variants of rate law.

Rate law for the reaction system

The three different variants of equation (5) take the following forms as a result of fitting of the kinetic data acquired during experimental study:

$$\text{RLA: } \frac{dC_P}{dt} = k_A \left(C_{A_0} - \frac{C_P}{6} \right) (C_{B_0} - C_P) \quad (18)$$

$$\text{RLB: } \frac{dC_P}{dt} = k_B \left(C_{A_0} - \frac{C_P}{6} \right)^{0.9590} (C_{B_0} - C_P)^{0.9111} \quad (19)$$

$$\text{RLC: } \frac{dC_P}{dt} = k_C \left(C_{A_0} - \frac{C_P}{6} \right) (C_{B_0} - C_P)^{0.7455} \quad (20)$$

In the equations (18) – (20), k_A , k_B and k_C are the observed rate constants for RLA, RLB and RLC respectively. The predictive capability of RLA, RLB and RLC can be assessed in Fig. 7 where experimental rates have been plotted against predicted values thereof. Although there is somewhat larger scatter in the middle of the Fig but the majority of the points in each case fall well between the convincing limits of $\pm RMSD$ (dot-dashed lines) around the ideal response (black dotted line). In each case F_{ratio} between mean sum of squares for regression to mean sum of squares for residuals is favorably large such that $p_{KMA} = p_{KMB} = p_{KMC} = 0$ (Table 3–5). This suggests that amount of variability explained by regression is far greater than the amount due to residual error in every case; therefore every model is statistically representing strong correlation between experimental and predicted rates.

However, discrimination among different rate laws is possible on the basis of $RMSD$, F_{ratio} and R^2 values. As $RMSD_{RLA} > RMSD_{RLB} > RMSD_{RLC}$, $F_{RLA} < F_{RLB} < F_{RLC}$ and $R^2_{RLA} < R^2_{RLB} < R^2_{RLC}$, so RLA has the widest deviations from the ideal response and has the least statistical significance, whereas RLC is the most significant in the statistical sense with RLB having the intermediate significance. Therefore on the basis of statistical comparison, RLC is the optimum choice as a representative rate law of the reaction system.

In Fig. 7 the solid lines of best fit for RLA (black) and RLB (blue) somewhat deviates on both the ends from the ideal response with the deviation for RLA being slightly larger than RLB. These deviations are relatively higher on the end

corresponding to higher rates that are achieved near the start of the reaction where the concentration of Co(III) is much lower. This is a manifestation of the fact that both RLA and RLB are rather incapable of describing the kinetic behavior of the reaction system near the start of the reaction that is usually the most important region in a kinetic profile.

On the other hand in case of RLC the red solid bold line of best fit excellently overlaps the ideal response and actually makes an angle of 45° with the horizontal. This is indicative of the fact that RLC is well capable of representing the kinetic fingerprint of the reaction system throughout from start to end.

Additionally the residuals in all the cases follow the classical normal distribution (Fig. 8). However, the distinct feature for RLA and RLB is that for both rate laws the numbers of positive residuals are higher than negative ones and this effect is more prominent in RLA. On the other hand, in case of RLC the distribution of residuals on either sides of an essentially zero mean ($1.498E - 9 \approx 0$) is pretty uniform with the peak corresponding to a normal probability density value of 25020. Consequently cumulative probability density curve for RLC exactly passes through the central point (0, 0.5) and is symmetrical around a zero mean. The peak values of the normal probability densities for RLA and RLB are 22825 and 23605 respectively that are definitely low as compared to the value for RLC and cumulative distribution curves also do not pass through the center. Further standard deviation (SD) of residuals has the smallest value for RLC ($SD_{RLA} > SD_{RLB} > SD_{RLC}$). These properties of residuals also favor in the selection of RLC as the representative, most precise and highly probable rate law for the reaction system.

Comparison of computed reaction profiles and surfaces

The experimental points in Fig. 9 were collected at 358.15K and at the center of DOE for set 1, 34, 35, 36 and 37. The solutions, of RLA (black curve, $R^2 = 0.9318$), RLB (blue curve, $R^2 = 0.9345$) and RLC (red curve, $R^2 = 0.9367$), in each case captures more than 93% of the variation in the experimental data. The trend in R^2 values is still the same i.e., $R^2_{RLA} < R^2_{RLB} < R^2_{RLC}$. Therefore red curve for RLC is the best possible representation of the experimental kinetic data especially during the

early stages of the reaction system up to 60 seconds. The illustration also depicts the experimentally fitted general exponential model (dashed curve) for making a contrast with the various alternatives for rate law and it is evident that the rate originally calculated using general exponential model, for fitting purpose, were quite reasonable throughout the range studied and especially in the early stages of the reaction that is usually the most important region from the kinetic perspective. Nevertheless, the general exponential model was unable to pass exactly through the origin as do other variants of the rate law. Not only has each variant passed through the origin but up to 13 seconds there was no significant difference among them. The considerable deviation starts after 13 seconds and begins to widen as time increases.

The computed response surfaces of the reaction system have been prepared through solutions of rate laws (18) – (20) and can be observed in Fig. 10. This is a 3D representation of the computed reaction profiles for almost the entire ranges for time and temperature studied experimentally. As can be seen, there is an excellent replica of the kinetic response of the reaction system at various temperatures. Again the significance of response surfaces is in the ascending order from RLA – RLC.

Arrhenius & Eyring analyses

Numerical values of the observed rate constant k for various rate laws and their graphical representations against absolute temperature can be seen in Fig. 11. The observed rate constants k (for a wide temperature range from 298.15 – 363.15K) were determined using A_a and E_a estimates for the Arrhenius equation. The curves of observed rate constant follow the classical Arrhenius shape.⁵³ Accordingly the plots of $\ln k$ against $1/T$ are straight lines (Fig. 12). Hence the selection of Arrhenius equation, as a model for dependence of rate constant on absolute temperature, was a sensible choice during development of rate law (section 2). Comparison of Arrhenius and Eyring equations reveals that:

$$A_a \equiv \frac{k_B T}{h} e^{\frac{\Delta S^\ddagger}{R}} \quad (21)$$

$$E_a \equiv \Delta H^\ddagger \quad (22)$$

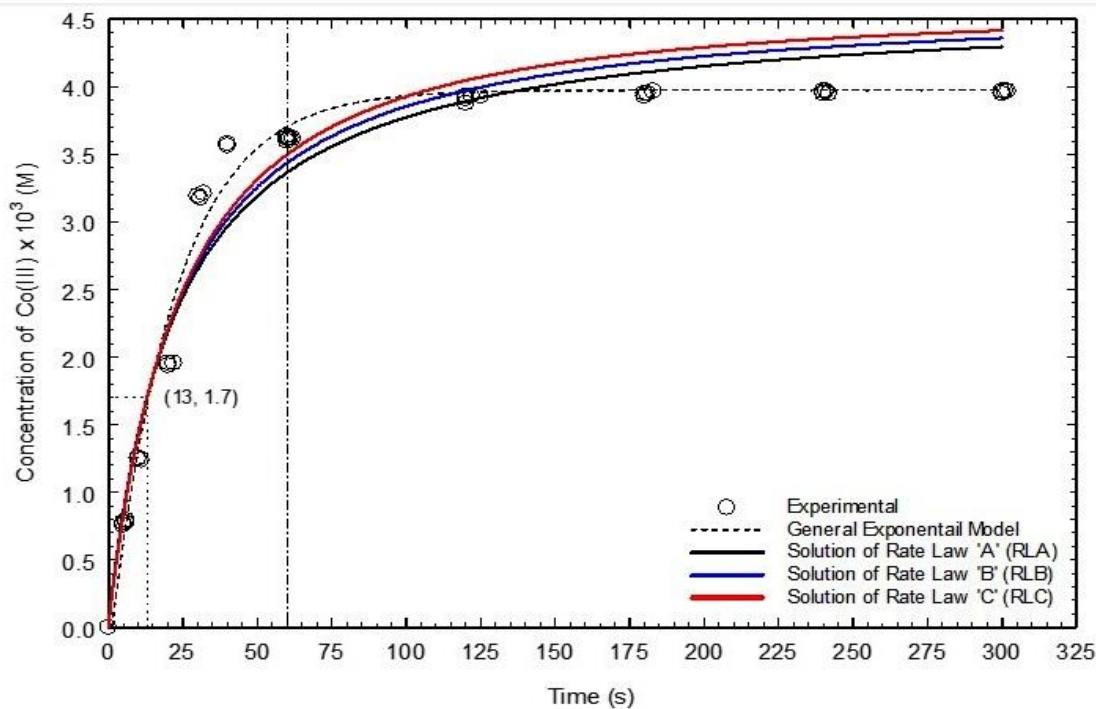


Fig. 9: Comparison of computed reaction profiles for different variants of rate law at 85°C for set 1, 34, 35, 36 and 37 of the DOE.

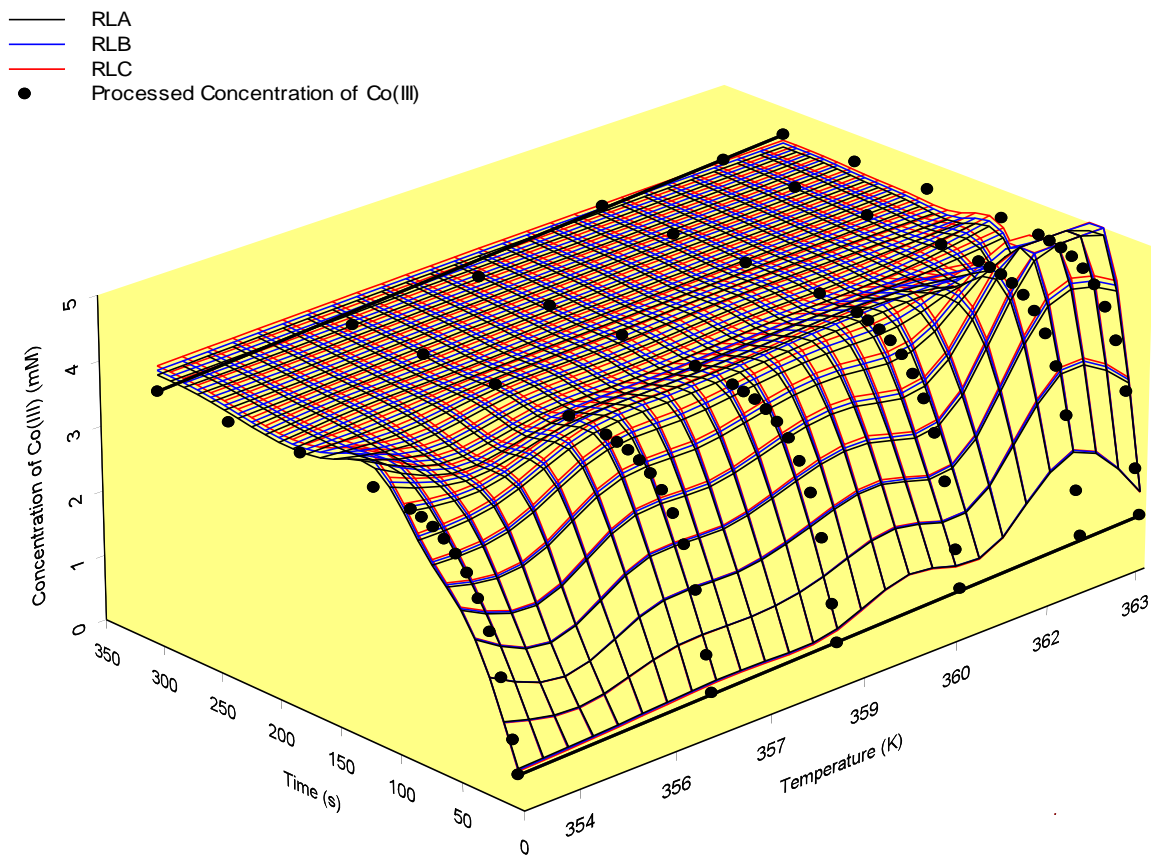


Fig 10: Comparison of computed response surfaces for different variants of rate law at the center of DOE

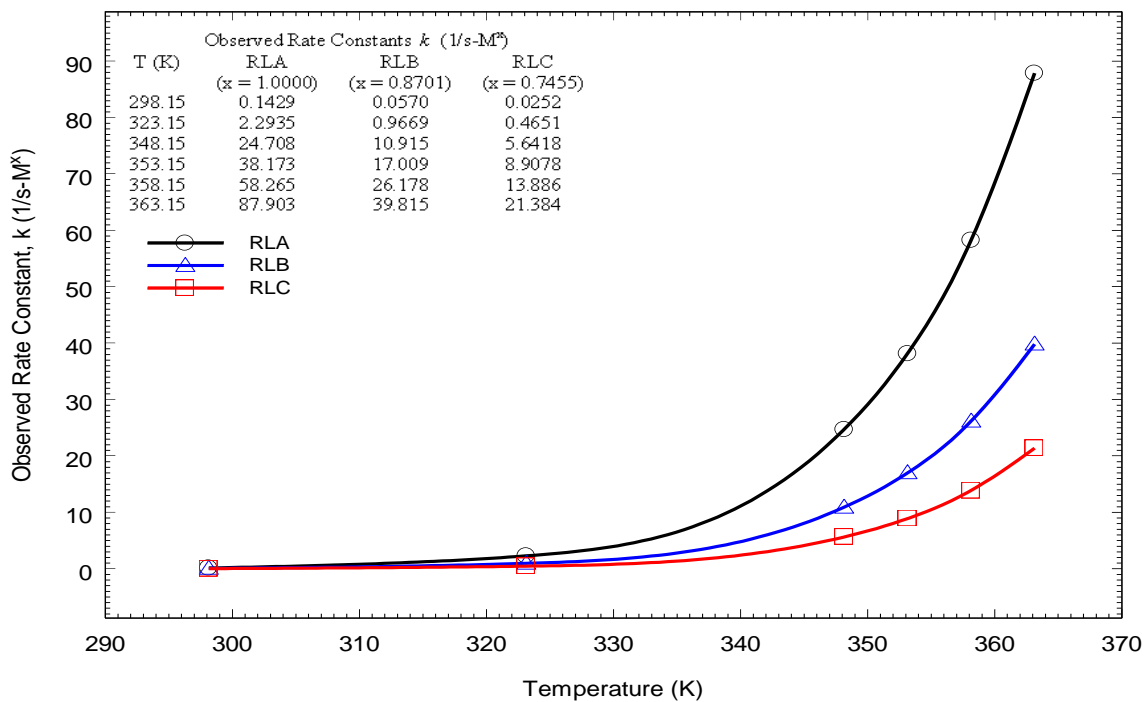


Fig 11: Variation in the observed rate constant against absolute temperature for different variants of rate law

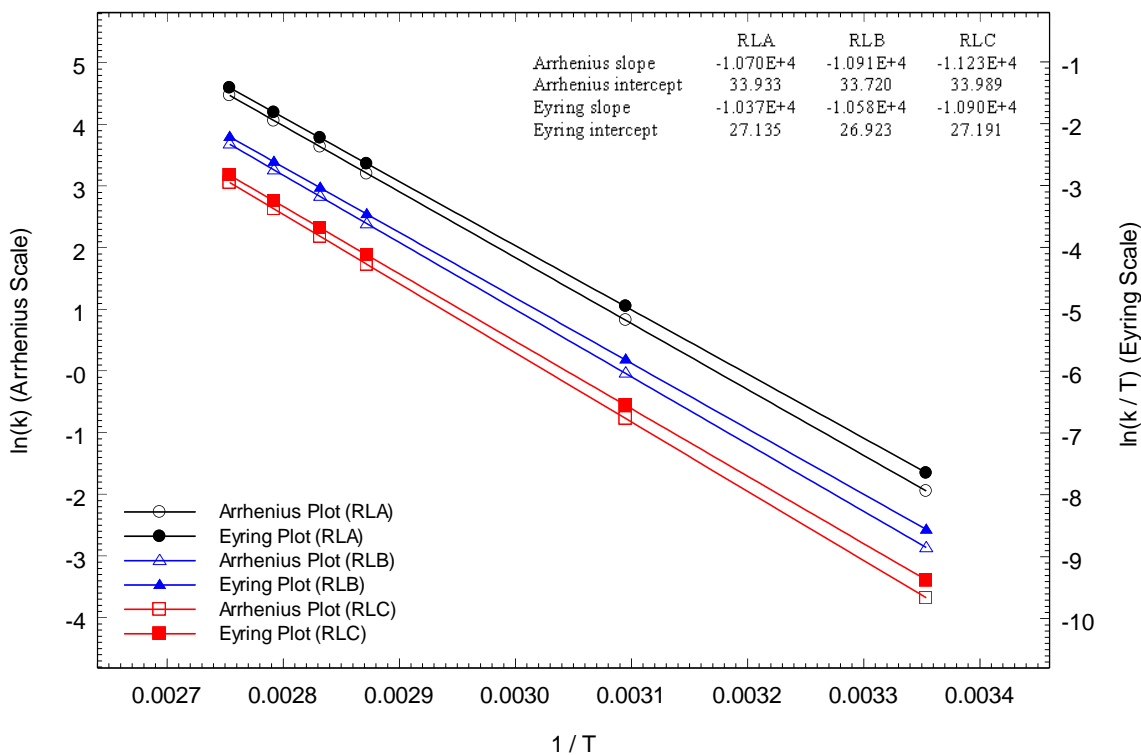


Fig 12: Arrhenius & Eyring analyses of observed rate constants for different variants of rate law.

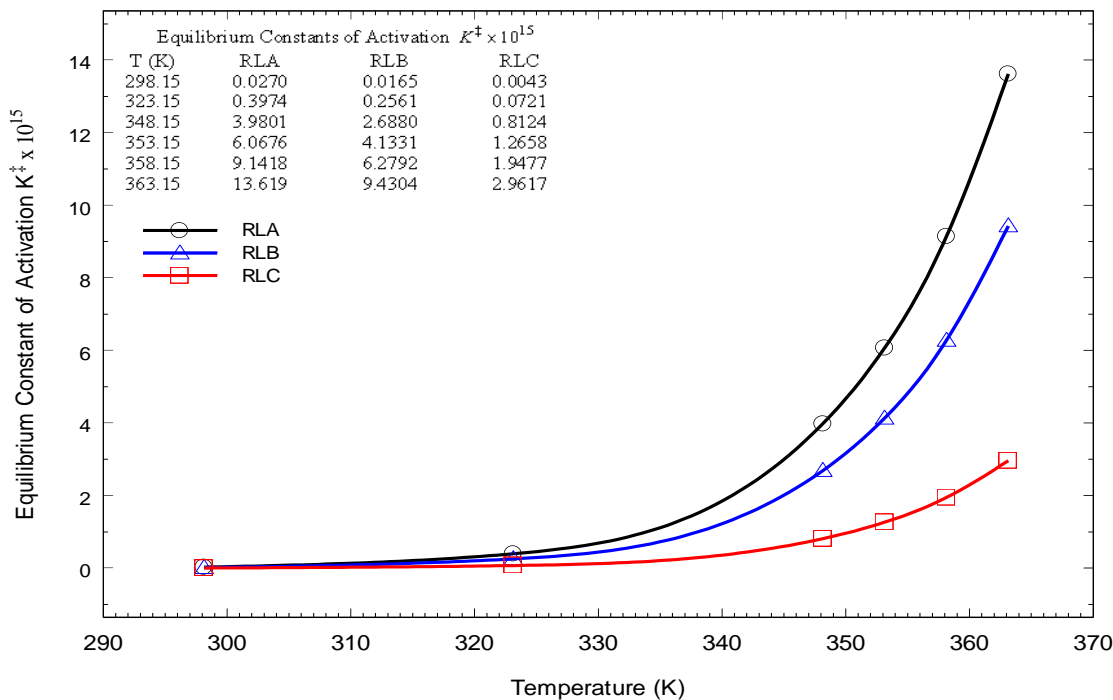


Fig. 13: Variation in equilibrium constant of activation against absolute temperature for different variants of rate law.

Therefore the absolute relative error (*ARE*) between the energy of activation estimated from Arrhenius equation and the estimated standard enthalpy of activation ΔH^\ddagger from Eyring equation must not be significant and this can be observed for various rate laws in Table 2 where the *ARE* is < 3.1%. For a reaction in solution carried out at different absolute temperatures, the relation between E_a and ΔH^\ddagger could be described by:[46]

$$\bar{E}_a = \text{mean}(\Delta H^\ddagger + RT) \quad (23)$$

Hence for a range of temperatures the *ARE* between energy of activation estimated from Arrhenius Equation and that of the mean activation energy estimated from equation (23), should also be trivial. Comparable results, where *ARE* is < 0.12%, can be observed in Table-2. Overall minimum *ARE* in either case are for RLC.

The values for the standard entropy of activation ΔS^\ddagger can also be seen in Table 2, which are rationally negative. Standard entropy of activation gives much useful information about the nature of the reaction and about the activated complex. First of all if $\Delta S^\ddagger < 0$ the reaction will be slow as is the reaction system studied during present research. Further in case of complex reactants, such as Co(II) and chlorate, there is usually considerable rearrangement of energy among various degrees of freedom during the formation of activated complex and thereby there is always a decrease in the entropy. The sign and magnitude of ΔS^\ddagger also provide clues about the molecularity of the rate determining step in a reaction. Low to moderately negative values for ΔS^\ddagger indicates that entropy decreases on forming activated complex that pointed out an associative mechanism for the formation of activated complex [54]

The values of estimated K^\ddagger and its pictorial representation against absolute temperature can be seen in Fig. 13. The curves clearly indicate that at temperatures below 348.15K, K^\ddagger is relatively negligible, as compared to its values for higher temperatures. The activated complex forms during the first step in a chemical reaction, subsequently decomposes to form products. Comparatively low values of K^\ddagger below 348.15K suggest that the concentration of activated complex would be very small and hence formation of products is extremely

slow at low temperatures. This is the reason why at temperatures below 348.15K the rate of reaction is insignificantly slow (Fig. 6).

Precision of estimated rate constants

In the light of the foregoing discussion the rate of the reaction system may be best described by the following rate law:

$$r = kC_A C_B^{0.7455} \quad (24)$$

By rearrangement and taking logarithms:

$$\ln k = \ln r - \ln C_A - 0.7455 \ln C_B \quad (25)$$

In this relation the dependent variable is k and independent variables are r , C_A and C_B , all of which are experimental quantities. The observed rate constant k is indirectly estimated from the estimated values of Arrhenius equation parameters. The precision values for both r and C_P are known. Since C_A and C_B are functions of C_P through stoichiometric relations, the precision of C_A and C_B will be equal to that of C_P . With these information in hand the fractional error or precision of the observed rate constants k for the reaction system may be defined as: [55-57]

$$\left(\frac{\Delta k}{k}\right)^2 = \left(\frac{\partial \ln k}{\partial \ln r}\right)^2 \left(\frac{\Delta r}{r}\right)^2 + \left(\frac{\partial \ln k}{\partial \ln C_A}\right)^2 \left(\frac{\Delta C_A}{C_A}\right)^2 + \left(\frac{\partial \ln k}{\partial \ln C_B}\right)^2 \left(\frac{\Delta C_B}{C_B}\right)^2 \quad (26)$$

The squares of the partial derivatives in equation (26) are derived from partial differentiation of equation (25):

$$\left(\frac{\partial \ln k}{\partial \ln r}\right)^2 = \left(\frac{\partial \ln k}{\partial \ln C_A}\right)^2 = 1 \quad \& \quad \left(\frac{\partial \ln k}{\partial \ln C_B}\right)^2 = 0.7455^2$$

The fractional errors in C_P and r have been estimated and given in Figs 4 and 8:

$$\frac{\Delta r}{r} = 1.594 \times 10^{-5} \quad \&$$

$$\frac{\Delta C_P}{C_P} = \frac{\Delta C_A}{C_A} = \frac{\Delta C_B}{C_B} = 1.761 \times 10^{-4}$$

$$\text{Hence, } \frac{\Delta k}{k} = 2.2023 \times 10^{-4}$$

This result shows that the observed rate constants for the reaction system have an extremely remarkable precision of 0.02 %.

Conclusion

Following conclusions may be drawn on the basis of extensive experimental and modeling study of the reaction system:

The kinetic behavior of the electron transfer reaction between Co(II) and chlorate ions in acetic acid solution may be best described by the rate law: $r = kC_A C_B^{0.7455}$. According to the rate law the order with respect to chlorate is 1 but the consumption of Co(II) follows a fractional order. No simple mechanism could be postulated for such a complex kinetic behavior. Further investigations are required for the establishment of the detailed mechanism. The observed rate constant has a remarkable precision of 0.02 %, which is indicative of highly precise experimental study. Arrhenius and Eyring equations are the models of choice for describing the effect of temperature on observed rate constants. The formation of activated complex follows an associative mechanism. The rate law may be used for every practical purpose such as to design a reactor for an industrial, pilot plant or laboratory scale operation.

Nomenclature

| | |
|-------------------|---|
| R | Universal gas constant, J/mol-K |
| k_B | Boltzmann constant, J/K |
| h | Planck constant, J-s |
| T | Absolute temperature, K |
| t_{Exp} | Experimental reaction time, s |
| t | Reaction time, s |
| C_{A_0} | Initial concentration of chlorate in reaction mixture, M = mol/L |
| C_A | Concentration of chlorate in reaction mixture at time t , M |
| C_{B_0} | Initial concentration of Co(II) in reaction mixture, M |
| C_B | Concentration of Co(II) in reaction mixture at time t , M |
| $C_{P_{Exp}}$ | Experimental concentration of Co(III) in reaction mixture at time t , M |
| C_P | Processed concentration of Co(III) in reaction mixture at time t , M |
| $C_{S_2O_3^{-2}}$ | Concentration of standard sodium thiosulfate, M |
| r | Rate of production of Co(III), M/s |
| $V_{S_2O_3^{-2}}$ | Volume of standard sodium thiosulfate, mL |
| V_{RM} | Volume of reaction mixture, mL |
| k | Observed rate constant, 1/s-M ⁿ |

| | |
|----------------------|--|
| A_a | Pre-exponential factor in Arrhenius equation, 1/s-M ⁿ |
| E_a | Energy of activation in Arrhenius equation, J/mol |
| ΔG^\ddagger | Standard free energy change of reaction, J/mol |
| ΔH^\ddagger | Standard enthalpy change of reaction, J/mol |
| ΔS^\ddagger | Standard entropy change of reaction, J/mol-K |
| K^\ddagger | Equilibrium constant of activation |
| $RMSD$ | Root mean square deviation |
| SD | Standard deviation |
| R^2 | Coefficient of determination |
| F_{ratio} | F-statistics |
| <i>Greek Symbols</i> | |
| α | Order of reaction with respect to chlorate |
| β | Order of reaction with respect to Co(II) |

References

- G. N. Schrauzer, *Transition Metals in Homogeneous Catalysis*, Marcel Dekker, New York, (1971).
- G. W. Parshall, *Homogeneous Catalysis*, second ed., Wiley, New York, (1980).
- W. J. Mijs and C. R. H. I. De Jonge, *Organic Synthesis by Oxidation with Metal Compounds*, Plenum Press, New York, (1986).
- G. W. Parshall and S. D. Ittel, *Homogeneous Catalysis: The Applications & Chemistry of Catalysis by Soluble Transition Metal Complexes*, Wiley, New York, (1992).
- A. A. Wasim, S. Naz, M. N. Khan and S. Fazlur-rehman, Assessment of heavy metals in rice using atomic absorption spectroscopy, *Pak. J. Anal. Env. Chem.*, **20**, 67 (2019).
- A. E. Shilov and G. B. Shul'pin, Activation of C-H Bonds by Metal Complexes, *Chem. Rev.*, **97**, 2879 (1997).
- S. Bhaduri and D. Mukesh, *Homogeneous Catalysis: Mechanisms & Industrial Applications*, Wiley, New York, (2000).
- J. M. Brégeault, Transition-Metal Complexes for Liquid-Phase Catalytic Oxidation: Some Aspects of Industrial Reactions and of Emerging Technologies, *Dalton Trans.*, **17**, 3289 (2003).
- J. Reedijk and K. Poepelmeier, *Comprehensive Inorganic Chemistry II*, Elsevier, Oxford, (2013).
- A. E. Woodward and R. B. Mesrobian., Low Temperature Autoxidation of Hydrocarbons. The Kinetics of Tetralin Oxidation. *J. Am. Chem. Soc.*, **75**, 6189 (1953).
- Y. Kamiya, S. Beaton, A. Lafortune and K. U. Ingold., The Metal-Catalyzed Autoxidation of Tetralin: II. The Cobalt Catalyzed Autoxidation of Undiluted Tetralin and of Tetralin in Chlorobenzene. *Can. J. Chem.*, **41**, 2020 (1963).

12. E. I. Heiba, R. M. Dessau and W. J. Koehl Jr., Oxidation by Metal Salts. V. Cobaltic Acetate Oxidation of Alkylbenzenes. *J. Am. Chem. Soc.*, **91**, 6830 (1969).
13. Y. Kamiya and M. Kashima., The Autoxidation of Aromatic Hydrocarbons Catalyzed with Cobaltic Acetate in Acetic Acid Solution: I. The Oxidation of Toluene. *J. Catal.*, **25**, 326 (1972).
14. J. Hanotier, Ph. Camerman, M. Hanotier-Bridoux and P. De Radzitzky., Low-Temperature Oxidation of n-Alkanes by Cobaltic Acetate Activated by Strong Acids. *J. Chem. Soc., Perkin II*, 2247 (1972).
15. A. Onopchenko and J. G. D. Schulz., Oxidation by Metal Salts. *J. Org. Chem.*, **37**, 2564 (1972).
16. Y. Kamiya and M. Kashima., Autoxidation of Aromatic Hydrocarbons Catalyzed with Cobaltic Acetate in Acetic Acid Solution. II. Oxidation of Ethylbenzene and Cumene. *Bull. Chem. Soc. Jpn.*, **46**, 905 (1973).
17. A. Onopchenko and J. G. D. Schulz., Oxidation of n-Butane with Cobalt Salts and Oxygen via Electron Transfer. *J. Org. Chem.*, **38**, 909 (1973).
18. A. Onopchenko, J. G. D. Schulz., Electron Transfer with Aliphatic Substrates. Oxidation of Cyclohexane with Cobalt(III) Ions Alone and in the Presence of Oxygen. *J. Org. Chem.*, **38**, 3729 (1973).
19. J. Hanotier, M. Hanotier-Bridoux and P. De Radzitzky., Effect of Strong Acids on The Oxidation of Alkylarenes by Manganic and Cobaltic Acetates in Acetic Acid. *J. Chem. Soc., Perkin II*, 381 (1973).
20. Y. Kamiya and M. Kashima., Autoxidation of Aromatic Hydrocarbons Catalyzed with Cobaltic Acetate in Acetic Acid Solution. II. Oxidation of Ethylbenzene and Cumene. *Bull. Chem. Soc. Jpn.*, **46**, 905 (1973).
21. A. Onopchenko and J. G. D. Schulz., Electron Transfer with Aliphatic Substrates. Oxidations of Cycloaliphatic Substrates with Cobalt(III) and Manganese(III) Ions Alone and in The Presence of Oxygen. *J. Org. Chem.*, **40**, 3338 (1975).
22. L. Verstraelen, M. Lalmand, A. J. Hubert and P. Teyssie., Oxidation of Cyclic Hydrocarbons by Cobalt(III) Acetate. *J. Chem. Soc., Perkin II*, 1285 (1976).
23. C. F. Hendriks, H. C. A. van Beek, P. M. Heerthes, C. F. Hendriks, H. C. A. van Beek and P. M. Heertjes., The Oxidation of Substituted Toluenes by Cobalt(III) Acetate in Acetic Acid Solution. *Ind. Eng. Chem. Prod. Res. Dev.*, **17**, 256 (1978).
24. E. Baciocchi, L. Mandolini and C. Rol., Oxidation by Metal Ions. 6. Intramolecular Selectivity in the Side-Chain Oxidation of p-Ethyltoluene and Isodurene by Cobalt(III), Cerium(IV), and Manganese(III). *J. Org. Chem.*, **45**, 3906 (1980).
25. M. Harustiak, M. Hronec and J. Javsky., Kinetics and Mechanism of Cobalt Bromide Catalyzed Oxidation of p-Xylene in the Presences of Phase Transfer Catalyst. *J. Mol. Catal.*, **53**, 209 (1989).
26. P. Li and H. Alper., Mild Cobalt Chloride Catalyzed Benzylic Oxidation Under Neutral Conditions. *J. Mol. Catal.*, **61**, 51 (1990).
27. A. S. Goldstein and R. S. Drago., Oxidation of Alkanes by Cobalt(II) Salts of Weakly Coordinating Anions. *Inorg. Chem.*, **30**, 4506 (1991).
28. G. Falgayrac and A. Savall., Electrochemical Activation of the Catalytic Effect of Cobalt in Autoxidation of Toluene in Acetic Acid. *J. App. Electrochem.*, **29**, 253 (1999).
29. D. Bejan, J. Lozar, G. Falgayrac and A. Savall., Electrochemical Assistance of Catalytic Oxidation in Liquid Phase Using Molecular Oxygen: Oxidation of Toluenes. *Catal. Today*, **48**, 363 (1999).
30. S. M. D. Naqvi and F. Khan., Selective Homogeneous Oxidation System for Producing Hydroperoxides Concentrate: Kinetics of Catalytic Oxidation of Gas Oils. *Ind. Eng. Chem. Res.*, **48**, 5642 (2009).
31. S. M. D. Naqvi, M. A. Kamal and F. Khan., Selective Homogeneous Oxidation System for Producing Hydroperoxides Concentrate: Kinetic Simulation of Catalytic Oxidation of Gas Oils. *Ind. Eng. Chem. Res.*, **49**, 7210 (2010).
32. S. M. D. Naqvi., *Catalytic oxidation of gas oil: Kinetic analyses & simulation*, Scholars Press, Saarbrucken, (2012).
33. S. M. D. Naqvi, M. A. Kamal, S. M. R. Kazmi, K. Riaz and F. Khan., Liquid Phase Homogeneous Catalytic Oxidation of Gas Oil: Elucidation of Complex Chemical Transformation Network. *J. Basic Appl. Sci.*, **11**, 136 (2015).
34. P. J. Proll, L. H. Sutcliffe and J. Walkley., Species of Cobalt(II) in Acetic Acid. Part I. Cobaltous Acetate in the Presence of Water and of Sodium Acetate. *J. Phys. Chem.*, **65**, 445 (1961).
35. S. S. Lande, C. D. Falk and J. K. Kochi., Cobalt(III) Acetate from the Ozonation of Cobaltous Acetate. *J. Inorg. Nucl. Chem.*, **33**, 4101 (1971).
36. K. Sawada and M. Tanaka., Aquation of some Transition Metal Acetates in Acetic Acid. *J. Inorg. Nucl. Chem.*, **35**, 2455 (1973).

37. C. F. Hendriks, H. C. A. van Bech and P. M. Heerthes., The Structure of Cobalt(II) Acetate and Cobalt(III) Acetate in Acetic Acid Solution. *Ind. Eng. Chem. Prod. Res. Dev.*, **18**, 43 (1979).
38. A. B. Blake, J. R. Chipperfield, S. Lau and D. E. Webster., Studies on the Nature of Cobalt (III) Acetate. *J. Chem. Soc. Dalton Trans.*, 3719 (1990).
39. D. E. Babushkin and E. P. Talsi., Multinuclear NMR Spectroscopic Characterization of Co(III) species: Key Intermediates of Cobalt Catalyzed Autoxidation. *J. Mol. Catal. A.*, **130**, 131 (1998).
40. W. Partenheimer., The Structure of Metal/Bromide Catalysts in Acetic Acid/Water Mixtures and its Significance in Autoxidation. *J. Mol. Catal. A.*, **174**, 29 (2001).
41. X. D. Jiao, P. D. Metelski and J. H. Espenson., Equilibrium and Kinetics Studies of Reactions of Manganese Acetate, Cobalt Acetate, and Bromide Salts in Acetic Acid Solutions. *Inorg. Chem.*, **40**, 3228 (2001).
42. H. Henschel, J. P. Klockner, I. A. Nicholls and M. H. Proseness., Computational and Structural Studies on the Complexation of Cobalt(II) Acetate by Water and Pyridine. *J. Mol. Struct.*, **1007**, 45 (2012).
43. S. Iwatsuki, K. Obeyama, N. Koshino, S. Funahashi, K. Kashiwabara, T. Susuki and H. D. Takagi. New Low-Spin Co(II) Complexes with Novel Tripodal 1,1,1-Tris(Dimethylphosphinomethyl)Ethane Ligand: Electron Transfer Kinetics and Spectroscopic Characterization of Co(II)P6 and Co(II)P3S3 Ions in Aqueous Solution. *Can. J. Chem.*, **79**, 1344 (2001).
44. K. J. Laidler., *Chemical Kinetics*, third ed., Pearson Education, New Delhi, (1987).
45. S. Glasstone., *Textbook of Physical Chemistry*, second ed., Jan de Lange, Deventer, (1946).
46. P. W. Atkins., *Physical Chemistry*, forth ed., Oxford University Press, Oxford, (1990).
47. I. M. Kolthoff, D. N. Hume., Determination of Iodate in the Presence of Bromate and Chlorate. *Ind. Eng. Chem.*, **15**, 174 (1943).
48. C. F. J. Wu and M. Hamada., *Experiments: Planning, Analysis, and Parameter Design Optimization*, Wiley, New York (2002).
49. R. G. Brereton., *Chemometrics: Data Analysis for the Laboratory and Chemical Plant*, Wiley, New York (2003).
50. R. Mezaki and J. R. Kittrell., Nonlinear Least Squares for Model Screening. *AIChE J.*, **14**, 513 (1968).
51. D. M. Bates and D. G. Watts., *Nonlinear Regression and its Applications*, Wiley, New York (1988).
52. H. S. Fogler., *Elements of Chemical Reaction Engineering*, forth ed. PHI Learning, New Delhi (2012).
53. A. A. Frost and R. G. Pearson., *Kinetics and Mechanism*, second ed., Wiley, Tokyo (1961).
54. J. H. Espenson., *Chemical Kinetics and Reaction Mechanisms*, second ed., McGraw Hill, New York (2002).
55. J. M. Smith., *Chemical Engineering Kinetics*, third ed, McGraw Hill, Singapore (1987).
56. G. Jeanmairet, B. Rotenberg, M. Levesque, D. Borgis and M. Salanne, A molecular density functional theory approach to electron transfer reactions, *Chem. Sci.*, **10**, 2130 (2019).
57. C. R. Dennis, G. J. van Zyl, E. Fourie, S. S. Basson and J. C. Swarts, A kinetic study of the oxidation of the tetrakis oxalatoironate (IV) ion by the hexacyanoferrate (III) ion in an oxalate buffer medium. *Reaction Kinetics, Mechanisms and Catalysis*, **132**, 599 (2021).
58. C. R. Dennis, E. Fourie, D. W. Margerum and J. C. Swarts, Kinetic advantage of inner sphere electron transfer reactions of copper (III, II) peptide complexes with cyano complexes of iron, molybdenum and tungsten. *Transition Metal Chemistry*, **45**, 147 (2020).